J Mater Sci (2009) 44:5017–5020
DOI 10.1007/s10853-009-3782-3

LETTER

Improvement of mechanical properties of hydroxyapatite particle-filled poly(L-lactide) biocomposites using lysine tri-isocyanate

Tetsuo Takayama · Mitsugu Todo

Received: 9 June 2009 / Accepted: 25 July 2009 / Published online: 4 August 2009

Poly(L-lactide) (PLLA) is known to be a bioabsorbable polymer with biocompatibility and therefore, has widely been used for bone fixation devices used in orthopedics and oral surgery [1, 2]. Blending with bioactive ceramics such as hydroxyapatite (HA) has recently been adopted to improve the bioactivity, the degradation rate and the stiffness of such medical devices [3–15]. It was, however, shown that the fracture properties of such HA/PLLA biocomposites tend to be much lower than those of neat PLLA mainly due to immediate failure along the interfaces between HA particles and PLLA matrix [16–18]. It was also recently discovered that lysine tri-isocyanate (LTI) effectively acts as a reactive additive for PLLA, and the bending strength, the modulus and the fracture toughness of PLLA are effectively improved due to LTI addition [19]. The aim of the present study was therefore to assess the effect of LTI addition on the microstructure and the mechanical properties of HA/PLLA composites.

HA particles (Sangi Co., Ltd.) with the representative size of about 5 μm were used as filler. HA particles and PLLA pellets (Toyota Motor Co., Ltd.) were mixed by a conventional melt-mixer at 190 °C. LTI was dry-blended with HA particles and PLLA pellets prior to the melt-mixing. The mixing ratio of HA and PLLA was fixed at 10:90 in weight fraction, and LTI content was chosen to be 2 phr [19]. Plates of 2 mm thick were then fabricated from the mixtures using a hot-press attached with a water-cooling system. These mixtures were melted at 180 °C and pressed at 30 MPa, and then quenched to room temperature using the cooling system. Single-edge-notch-bend (SENB) and beam specimens were prepared from the composite plates for mechanical testing. The specimen geometries are shown in Fig. 1. The crystallinity values of PLLA, $x_{c,PLLA}$, of HA/PLLA and HA/PLLA/LTI were measured using a differential scanning calorimeter. Three-point bending tests of the beam specimens were performed at a loading rate of 10 mm/min using a servohydraulic testing machine. The bending modulus, E, and the bending strength, σ_f, were then calculated from the linear potion of the load–displacement curve and the maximum load, respectively, using the following formulae:

$$E = \frac{L^3}{4wb^3}S \text{ and } \sigma_f = \frac{3PL}{2wb^2} \quad (1)$$

where S, L, w, b and P are the initial slope of the load–displacement curves, the span length, the width, the thickness and the maximum load, respectively. Three-point bending tests of the SENB specimens were also conducted at a loading rate of 1 mm/min, and the J-integral value at crack initiation, J_{in}, was evaluated as the mode I fracture energy using the following formula:

$$J_{in} = \frac{\eta U_{in}}{W(B-a)} \quad (2)$$

where B, W and a are the thickness, width and the initial crack length of the SENB specimen, respectively, and η the geometrical correction factor, which is equal to 2 for the standard SENB specimen. U_{in} is the critical energy defined as the area under the load–displacement curve up to the crack initiation point at which the rigidity of the SENB specimen decreased rapidly. Fracture surfaces of the SENB specimens were observed using a field emission scanning electron microscope (FE-SEM).

T. Takayama
Graduate School of Science and Engineering, Yamagata University, Yonezawa, Yamagata 992-8510, Japan

M. Todo (✉)
Research Institute for Applied Mechanics, Kyushu University, 6-1 Kasuga-koen, Kasuga, Fukuoka 816-8580, Japan
e-mail: todo@riam.kyushu-u.ac.jp

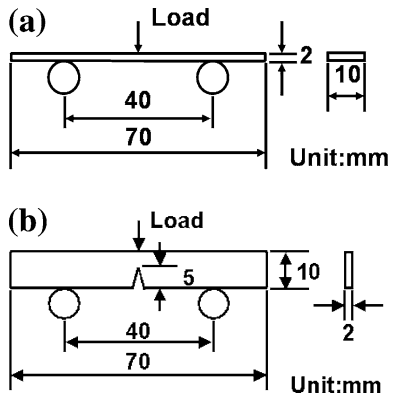

Fig. 1 Specimen geometries. **a** Three-point bend specimen, **b** mode I fracture specimen

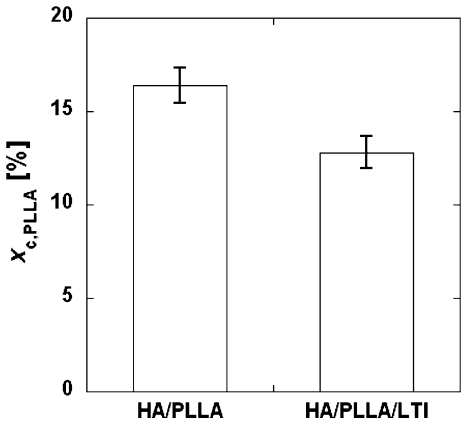

Fig. 2 Effect of LTI on the crystallinity of PLLA, $x_{c,PLLA}$

The crystallinity of PLLA, $x_{c,PLLA}$ are shown in Fig. 2. It is noted that $x_{c,PLLA}$ tends to decrease by LTI addition. This implies that crystallization of PLLA is hindered by crosslinking of PLLA molecules induced by chemical reaction between the hydroxyl group of PLLA and the isocyanate group of LTI [19]. It is also considered that the improvement of HA–PLLA interfacial connection due to LTI addition may affect the reduction of crystallization by constraining the mobility of PLLA molecules. Typical load–displacement curves obtained from the three-point bending tests of the beam specimens are shown in Fig. 3. It is clearly seen that the maximum load and the corresponding displacement of HA/PLLA/LTI were greater than those of HA/PLLA, clearly indicating the effectiveness of LTI addition for bending mechanical behaviour. E and σ_f values calculated by Eq. 1 are shown in Fig. 4. E and σ_f of HA/PLLA/LTI becomes larger than those of HA/PLLA. It should be noted that E and σ_f of HA/PLLA/LTI are also greater than those of neat PLLA ($E = 4$ GPa and $\sigma_f = 120$ MPa), although σ_f of HA/PLLA is smaller than that of PLLA. The crosslinking reaction of PLLA macromolecules with LTI results in these improvements of the

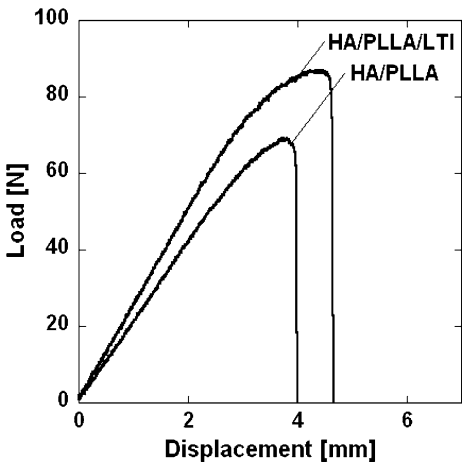

Fig. 3 Typical load–displacement curves obtained from bending mechanical tests

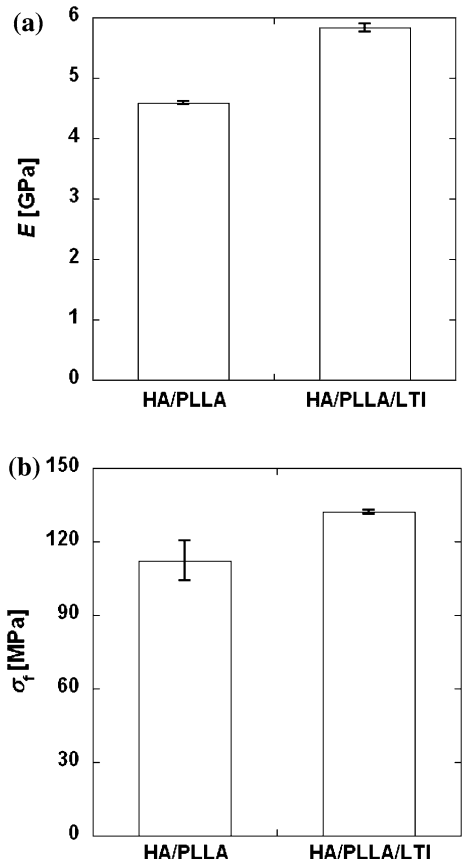

Fig. 4 Effect of LTI on the bending mechanical properties. **a** Bending modulus, **b** bending strength

bending properties. Typical load–displacement curves obtained from three-point bending tests of SENB specimen are shown in Fig. 5. It is clearly seen that the maximum load and the corresponding displacement of HA/PLLA/LTI are greater than those of HA/PLLA. J_{in} values obtained

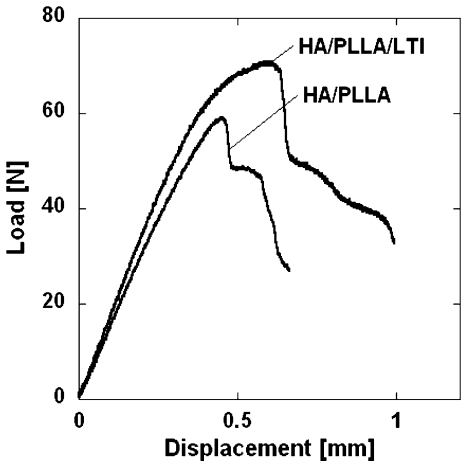

Fig. 5 Typical load–displacement curves obtained from mode I fracture tests

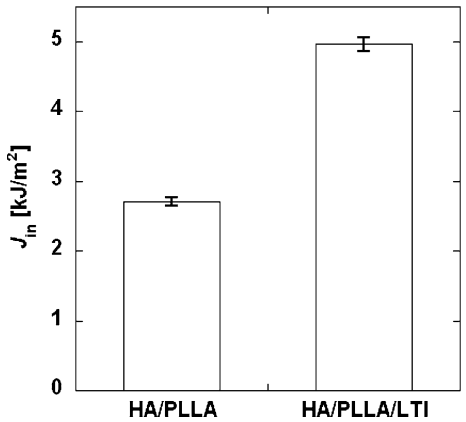

Fig. 6 Effect of LTI on the mode I fracture energy, J_{in}

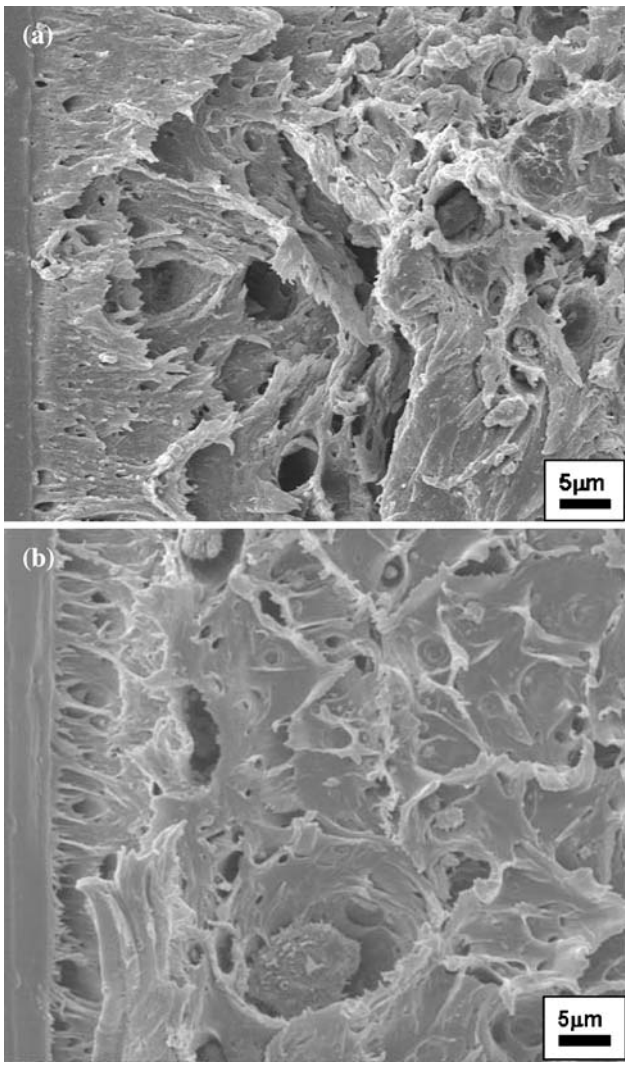

Fig. 7 FE-SEM micrographs of fracture surfaces in notch-tip region. **a** HA/PLLA, **b** HA/PLLA/LTI

from Eq. 2 are shown in Fig. 6. It is noted that J_{in} of HA/PLLA/LTI becomes greater than that of neat PLLA ($J_{in} = 3.5$ kJ/m^2). It is shown that J_{in} of HA/PLLA/LTI is increased by 82% due to LTI addition. It has been found from our previous study that LTI addition to pure PLLA increase the toughness of PLLA by 34%. This implies that the interfacial modification may be more effective on the improvement of J_{in}. It is thus concluded that LTI effectively improves both the bending mechanical properties, the modulus and the strength, and the mode I fracture energy.

FE-SEM micrographs of the mode I fracture surfaces of HA/PLLA and HA/PLLA/LTI are shown in Fig. 7. The fracture surface of HA/PLLA is characterised by rough surface with void formation. The voids are thought to be created by debonding HA particles from PLLA matrix. These voids cause local stress concentration in the surrounding regions, resulting in accelerated fracture initiation and therefore reduction of fracture energy. On the other hand, HA/PLLA/LTI shows less void formation, indicating improved interfacial bonding strength between HA particles and PLLA matrix. This interfacial modification is also clearly indicated by Fig. 8. In HA/PLLA/LTI, PLLA molecular bundles are firmly connected into the surface of the HA particle. On the contrary, there is no such interconnection in HA/PLLA.

In summary, effect of LTI addition on the bending mechanical properties and the mode I fracture energy of HA/PLLA was examined and the microstructural modification due to LTI was investigated. The bending modulus, the bending strength and the mode I fracture energy are effectively improved due to the crosslinking of PLLA macromolecules and the interfacial modification at the HA–PLLA interfaces by LTI addition.

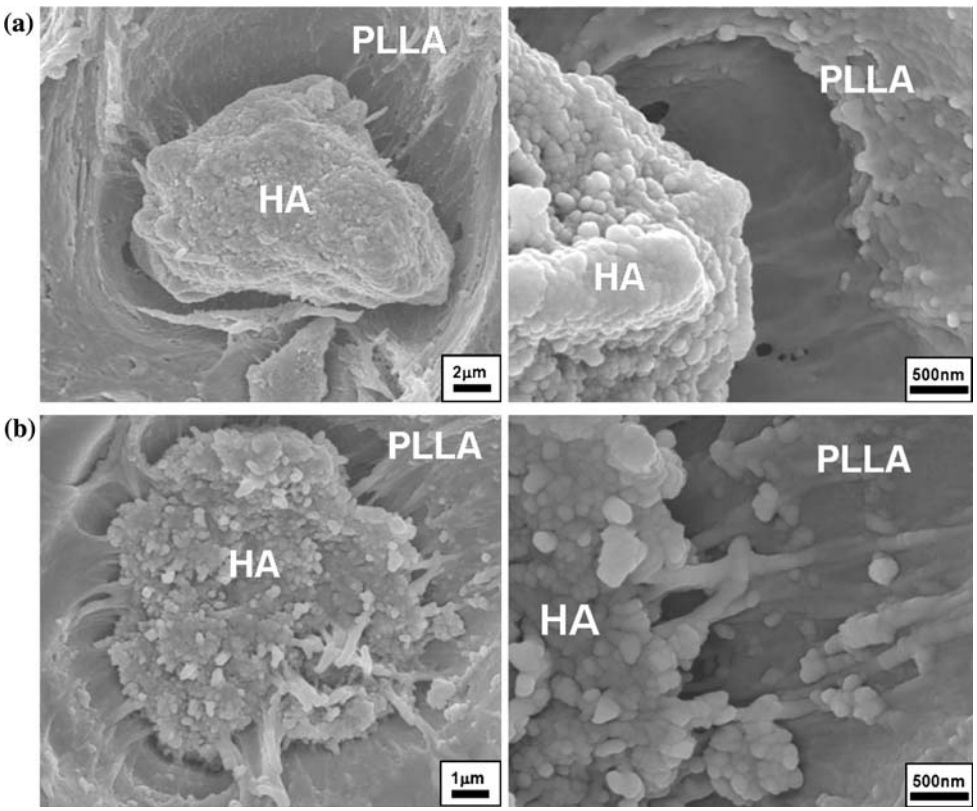

Fig. 8 Interfacial structure between HA particle and PLLA matrix. **a** HA/PLLA, **b** HA/PLLA/LTI

References

1. Leenslag JW, Pennings AJ, Bos RRM, Rozema FR, Boering J (1987) Biomaterials 8:70
2. Bostman OM (1991) J Bone Joint Surg 73-A:148
3. Shikinami Y, Okuno M (1999) Biomaterials 20:859
4. Yasunaga T, Matsusue Y, Furukawa T, Shikinami Y, Okuno M, Nakamura T (1999) J Biomed Mater Res 47:412
5. Kasuga T, Ota Y, Nogami M, Abe Y (2001) Biomaterials 22:19
6. Rizzi SC, Heath DJ, Coombes AGA, Bock N, Textor M, Downes S (1999) J Biomed Mater Res 47:475
7. Furukawa T, Matsusue Y, Yasunaga T, Nakagawa Y, Okada Y, Shikinami Y, Okuno M, Nakamura T (2000) J Biomed Mater Res 50:410
8. Furukawa T, Matsusue Y, Yasunaga T, Shikinami Y, Okuno M, Nakamura T (2000) Biomaterials 21:889
9. Deng X, Hao J, Wang C (2001) Biomaterials 22:2867
10. Shikinami Y, Matsusue Y, Nakamura T (2005) Biomaterials 26:5542
11. Hong Z, Zhang P, He C, Qiu X, Liu A, Chen L, Chen X, Jing X (2005) Biomaterials 26:6296
12. Debra DWC, Julia AK, Darinda MM, Cho LM (2006) J Biomed Mater Res Part A 78-A:541
13. Fang L, Yan J, Xiaodan L, Demin J (2006) J Appl Polym Sci 102:4085
14. Kikuchi M, Suetsugu Y, Tanaka J (1997) J Mater Sci-Mater Med 8:361
15. Verheyen CCPM, de Wijn JR, van Blitterswijk CA, de Groot K (1992) J Biomed Mater Res 26:1277
16. Todo M, Park SD, Arakawa K, Takenoshita Y (2006) Composites Part A 37:2221
17. Park SD, Todo M, Arakawa K, Takenoshita Y (2005) Key Eng Mater 297–300:2453
18. Todo M, Kagawa T (2007) J Mater Sci 43:799. doi:10.1007/s10853-007-2308-0
19. Todo M, Takayama T (2007) J Mater Sci 42:4712. doi:10.1007/s10853-007-1797-1